Environ. Sci. Technol. **2004**, *38,* 6676−6684

Reductive Dechlorination of Carbon Tetrachloride in Aqueous Solutions Containing Ferrous and Copper Ions

R. A. MAITHREEPALA AND RUEY-AN DOONG*

Department of Atomic Science, National Tsing Hua University, 101, Section 2, Kuang Fu Road, Hsinchu 30013, Taiwan

Fe(II) associated with iron-containing minerals has been shown to be a potential reductant in natural subsurface environments. While it is known that the surface-bound iron species has the capacity to dechlorinate various chlorinated compounds, the role of transition metals to act as catalysts with these iron species is of importance. We previously observed that the reduction of Cu(II) by Fe(II) associated with goethite enhanced the dechlorination efficiency of chlorinated compound. In this study, the reductive dechlorination of carbon tetrachloride (CCl_4) by dissolved Fe(II) in the presence of Cu(II) ions was investigated to understand the synergistic effect of Fe(II) and Cu(II) on the dechlorination processes in homogeneous aqueous solutions. The dechlorination efficiency of CCl_4 by Fe(II) increased with increasing Cu(II) concentrations over the range of 0.2−0.5 mM and then decreased at high Cu(II) concentrations. The efficiency and rate of CCl_4 dechlorination also increased with increasing dissolved Fe(II) concentration in the presence of 0.5 mM Cu(II) at neutral pH. When the Fe(II)/Cu(II) ratio varied between 1 and 10, the pseudo-first-order rate constant (k_{obs}) increased 250-fold from 0.007 h^{-1} at 0.5 mM Fe(II) to 1.754 h^{-1} at 5 mM Fe(II). X-ray powder diffraction and scanning electron microscopy analyses showed that Cu(II) can react with Fe(II) to produce different morphologies of ferric oxides and subsequently accelerate the dechlorination rate of CCl_4 at a high Fe(II) concentration. Amorphous ferrihydrite was observed when the stoichiometric Fe(II)/Cu(II) ratio was 1, while green rust, goethite, and magnetite were formed when the molar ratios of Fe(II)/Cu(II) reached 4−6. In addition, the dechlorination of CCl_4 by dissolved Fe(II) is pH dependent. CCl_4 can be dechlorinated by Fe(II) over a wide range of pH values in the Cu(II)-amended solutions, and the k_{obs} increased from 0.0057 h^{-1} at pH 4.3 to 0.856 h^{-1} at pH 8.5, which was 9−25 times greater than that in the absence of Cu(II) at pH 7−8.5. The high reactivity of dissolved Fe(II) on the dechlorination of CCl_4 in the presence of Cu(II) under anoxic conditions may enhance our understanding of the role of Fe(II) and the long-term reactivity of the zerovalent iron system in the dechlorination processes for chlorinated organic contaminants.

* Corresponding author phone: +886 3 5726785; fax: +886 3 5718649; e-mail: radoong@mx.nthu.edu.tw.

Introduction

Chlorinated hydrocarbons such as carbon tetrachloride (CCl_4), chloroform ($CHCl_3$), and trichloroethylene are the most frequently found contaminants in soil and groundwater (*1*, *2*). Because they are prevalent in contaminated sites and are highly toxic to human beings and ecosystems, studies have been conducted to elucidate the kinetics and mechanisms of dechlorination of these compounds in the contaminated sites (*3*, *4*). The rapid dechlorination of chlorinated hydrocarbons in the presence of Fe(II) species, acting as environmental reductants under anoxic conditions, has recently been reported (*5*−*10*). Fe(II) species can be present in the subsurface environment in a wide variety of forms including dissolved, soluble complexes, surface-bound, and as a structural component in Fe(II)-bearing minerals (*11*). Studies showed that ferrous ion associated with Fe(III)-containing minerals can significantly reduce several pollutants including nitroaromatics polyhalogenated alkanes, chloroamine compounds, and carbamate pesticides (*5*−*10*, *12*−*17*). The degradation rate and efficiency is dependent on the environmental conditions such as pH value, surface density of Fe(II), available surface area of ferric oxides, and the presence of transition metal ions.

Besides the surface-bound iron species, the dissolved ferrous species is also a ubiquitous component in contaminated groundwater and plays an important role in redox processes under the reducing environments (*18*, *19*). Aqueous Fe(II) is also known as a reducing agent that can effectively reduce inorganic ions such as Tc(VII) and Cr(VI) as well as organic pollutants (*20*, *21*). Doong and Wu (*22*) showed that it is thermodynamically possible for Fe(II) to dechlorinate CCl_4 with a relatively long incubation time of 33 d. Elsner et al. (*23*) reported that hexachloroethane (HCA) can be dechlorinated by dissolved Fe(II) under anoxic conditions at pH 7.2 (*10*). However, the dechlorination capability of aqueous Fe(II) is usually orders of magnitude lower than that of surface-bound Fe(II) species (*10*). More recently, studies demonstrated the catalytic activity of transition metals species in the reduction of a range of contaminants by a number of bulk reductants (*9*, *11*, *24*). Our previous work (*9*) showed that the reduction of Cu(II) to Cu(I) by Fe(II) associated with goethite (α-FeOOH) could produce cuprous oxide (Cu_2O) and amorphous ferrihydrite ($Fe(OH)_3$), resulting in an increase in the dechlorination rate and efficiency of CCl_4. This observation suggests that Fe(II) could be oxidized to ferric oxides and oxyhydroxides by Cu(II) to form surface-bound iron species and thus gives impetus to use Cu(II) to enhance the reactivity of dissolved Fe(II) in aqueous solutions for the dechlorination of the chlorinated hydrocarbons in Fe(II)-rich environments.

In natural subsurface environments, high concentrations of dissolved Fe(II) can be primarily generated from chemical and physical weathering, oxidation of pyrites and other iron-bearing minerals, and biological processes of reductive dissolution of ferric oxides and oxyhydroxides by dissimilatory iron-reducing bacteria (DIRB). Moreover, dissolved Fe(II) can be generated and released into the subsurface environment from the oxidation of metallic iron in permeable reactive barrier (PRB) systems. However, the role of Fe(II) in the reduction of chlorinated compounds is still unclear, especially when chlorinated hydrocarbons and transition metal ions coexist in the contaminated groundwater. Therefore, the objective of this study was to investigate the influence of Cu(II) ions on the reductive dechlorination of CCl_4 by aqueous Fe(II) species under anoxic condition. The effects of pH and concentrations of Fe(II) and Cu(II) on the dechlorination of

10.1021/es0493906 CCC: $27.50
Published on Web 11/12/2004

CCl_4 were also examined. Moreover, X-ray powder diffraction (XRPD) and scanning electron microscopy (SEM) were used to identify the crystal phases and the morphologies of the precipitates generated from the reaction of Fe(II) and Cu(II) in aqueous solutions.

Materials and Methods

Chemicals. All chemicals were used as received without further treatment. Carbon tetrachloride (CCl_4) (>99.8%, GC grade), chloroform ($CHCl_3$) (>99.8%, GC grade), and tris-(hydroxymethyl)aminomethane (TRIS buffer) (>99.8%), $CuCl_2 \cdot 2H_2O$ (99%) were purchased from Merck Co. (Darmstadt, Germany). $FeCl_2 \cdot 4H_2O$ (99%), $FeCl_3 \cdot 6H_2O$ (99%), *N*-(2-hydroxyethyl)piperazine-*N*′-2-ethanesulfonic acid (HEPES buffer) (>99.5%), 2-(*N*-morpholino)ethanosulfonic acid (MES buffer) (>99.5%), and sodium tartrate-2-hydrate ($C_4H_4Na_2O_6 \cdot 2H_2O$) (>99.5%) were purchased from Sigma-Aldrich Co. (Milwaukee, WI). Methylene chloride (DCM) (>99.8%, GC grade) and ethanol (HPLC grade) were obtained from J. T. Baker Co. (Philipsburg, NJ). Bathocuproinedisulfonic acid disodium salt ($C_{26}H_{18}N_2Na_2O_6S_2$) (90%) was purchased from Fluka (Buchs, Switzerland). All the solutions were prepared using distilled deionized water (Millipore, 18.3 mΩ) and were deoxygenated in vacuum-sealed bottles under an N_2 atmosphere (*9*, *25*, *26*).

Dechlorination Experiments. Batch experiments were conducted using 70 mL serum bottles filled with 50 mL of deoxygenated buffer solutions under anoxic conditions. Anoxic HEPES (50 mM) buffer solutions were used to control pH at 7.0 ± 0.1. Anoxic solutions were prepared by purging with N_2 (99.9995%) at a flow rate of 42 L min^{-1} in vacuum-sealed bottles. This process was repeated 4−5 times to remove trace amounts of oxygen in solution (*9*, *25*, *26*). Stock solutions of Fe(II) were prepared in 50 mL of deoxygenated buffer solutions and injected into the vacuum-sealed serum bottles after filtration through a 0.2 μm PTFE filter cartridge. The Fe(II) concentration in the filtrate was quantified by the ferrozine method at 562 nm (*9*, *26*). The stock solution of Cu(II) was prepared by dissolving $CuCl_2$ in deoxygenated deionized water in sealed serum bottles. Appropriate amounts of Fe(II) and Cu(II) stock solutions were introduced into the deoxygenated buffer solutions using N_2-purged plastic syringes to obtain final concentrations of 3 and 0.5 mM, respectively. For the pH effect experiment, 50 mM MES solutions were used for pH 5.5, 6.0, and 6.5. HEPES buffer was selected to maintain the pH at 7, 7.5, and 8.0, while TRIS buffer was used for pH 9. The concentration effects of Fe(II) and Cu(II) were also conducted by introducing various volumes of stock solutions into deoxygenated buffer solutions to get final concentrations ranging between 0.5 and 5.0 mM. All the reactor bottles were sealed with Teflon-lined rubber septa and aluminum crimp caps. After 20 h of equilibrium, an aliquot (50 μL) of the CCl_4 stock solution dissolved in anoxic methanol was delivered into serum bottles by a gastight glass syringe to obtain the final concentration of 20 μM CCl_4. Serum bottles were then incubated in an orbital shaker at 150 rpm maintained at 25 ± 1 °C in the dark. The total liquid volumes were maintained at 50 mL, resulting in a 20 mL headspace for headspace analysis. The headspace of the bottles was maintained under anoxic conditions by filling with a mixture of N_2 and Ar (80/20, v/v). Control experiments were also carried out without the addition of Fe(II) or Cu(II). All experiments were run in duplicate or triplicate.

Analytical Methods. The headspace analytical technique was used for the determination of chlorinated hydrocarbons (*9*, *25*). The concentrations of CCl_4 and the byproducts in the headspace of the test bottles were monitored by withdrawing 50 μL of gas in the headspace using a 100 μL gastight syringe. The mixture was then injected into a gas chromatograph (GC) (Perkin-Elmer, Autosystem) equipped with a flame ionization detector (FID) and an electron capture detector (ECD). A 60 m VOCOL fused-silica megabore capillary column (0.545 mm × 3.0 μm, Supelco Co.) was used to separate the chlorinated compounds. The column was connected to FID and ECD simultaneously by a Y-splitter with 40% of the flow (1.85 mL min^{-1}) to ECD to better identify and quantify the chlorinated hydrocarbons. The column temperature was isothermally maintained at 90 °C with nitrogen (>99.9995%) as the carrier gas. The relative standard deviation (RSD) for GC analysis was controlled within 10% in ECD and 5% in FID. The limits of detection (LODs) for CCl_4 and $CHCl_3$ were 0.04 and 0.1 μM, respectively. After headspace analyses, serum bottles were opened under N_2 atmosphere, and the pH and redox potential (ORP) were measured using a Microprocessor pH meter equipped with a pH electrode and ORP combination electrode.

XRPD was performed using an X-ray diffractometer (Regaku D/max-II B) and a Cu Kα radiation source (λ = 1.54056 Å) with 30 kV voltage and 20 mA current to identify the crystal phases of the precipitates. The precipitates were allowed to settle after the termination of the dechlorination experiment, and the supernatant was carefully removed from the sealed bottles using a N_2-purged syringe. After drying the precipitates using a gentle stream of N_2, samples were mounted on a glass sample holder using small amounts of grease. A drop of glycerol was immediately added to the mounted powder layer to minimize the exposure to air. The scan range for all samples was between 5 and 90° (2θ) at a scanning speed of 4°/min. Moreover, SEM (Topcon ABT-150s) was used to identify the morphology of the precipitates.

Concentrations of HCl-extractable Fe(II) in the serum bottles were monitored by withdrawing 0.5 mL of suspension using N_2-purged syringes and were immediately acidified with 1 M HCl (*26*). The acidified samples were centrifuged at 14000*g* for 10 min to remove particles, and the acid-extractable Fe(II) contents were analyzed using the ferrozine method at 562 nm (*9*, *26*). To determine the dissolved fraction of Fe(II) in serum bottles, aliquots were withdrawn with a 1 mL N_2-purged plastic syringe and then immediately filtered into an acidic solution using an acidified filter cartridge (0.2 μm). The concentration of the dissolved Fe(II) in the filtrate was determined by the ferrozine method, and the sorbed Fe(II) concentration was calculated from the difference between the total and dissolved concentrations. In addition, the total concentration of iron species was determined using an inductively coupled plasma optical emission spectrometer (ICP-OES) (Perkin-Elmer, Optima 3000XL).

The concentration of extractable Cu(I) was determined using the bathocuproinedisulfonic acid method with minor modifications (*27*). The aliquot was withdrawn by a 1 mL N_2-purged plastic syringe and was immediately added into the mixture containing 1 mL of 10% tartrate solution and 0.5 mL of 1% bathocuproinedisulfonic acid solution. After 30 min of reaction, the mixture was centrifuged at 14000*g* for 5 min. The Cu(I) concentration in the supernatant was then determined at 483 nm. Standard solutions of Cu(I) were prepared using 10% hydroxylammonium chloride as a reductant to reduce the $CuCl_2$ solution. The added Cu(II) concentration in the serum bottles was prepared based on the gravimetric concentration of $CuCl_2$ in the anoxic stock solution and was confirmed by ICP−OES analysis.

Results and Discussion

Concentration Effect of Cu(II) on CCl_4 Dechlorination in the Presence of 3 mM Fe(II). To understand the synergistic effect of aqueous Cu(II) and Fe(II) on the dechlorination of CCl_4 under anoxic conditions, the concentration effect of these divalent ions was evaluated. Figure 1 shows the dechlorination of CCl_4 as well as the change in pH and ORP

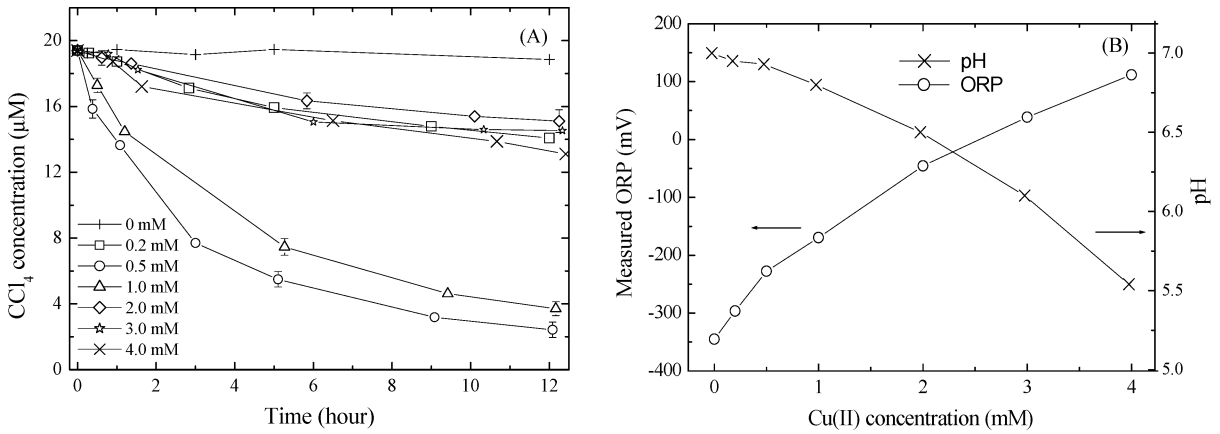

FIGURE 1. Effect of Cu(II) concentration on (A) the dechlorination of 20 μM CCl_4, and (B) the change in pH and ORP in anoxic buffered solution containing 3 mM Fe(II). HEPES (50 mM) was used to maintain the pH at 7.0 $\pm$ 0.1 in the Cu(II) concentration range of 0−0.5 mM. The decrease in pH at Cu(II) concentrations higher than 0.5 mM is due to the production of high concentrations of protons.

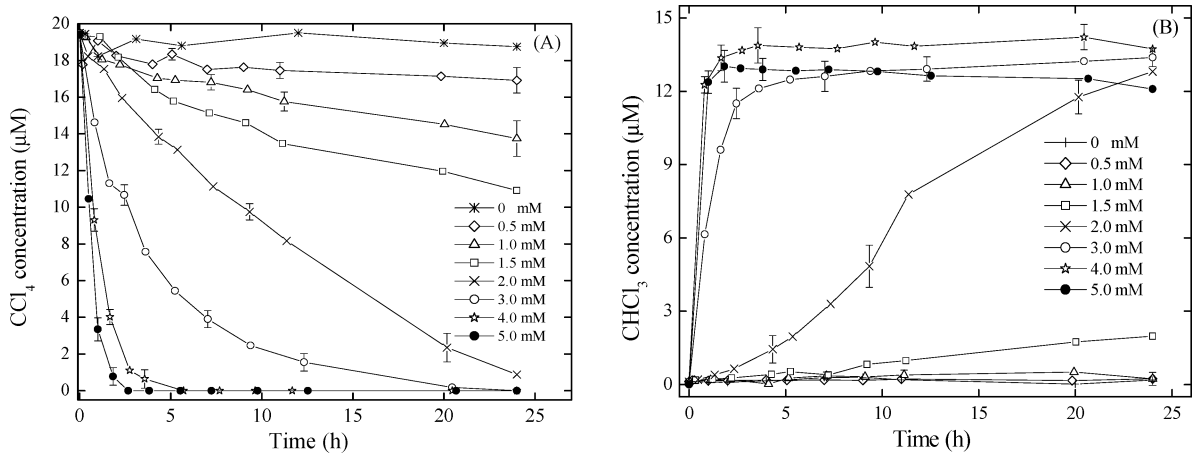

FIGURE 2. Effect of Fe(II) concentration on (A) the dechlorination of CCl_4 and (B) the production of $CHCl_3$ in the presence of 0.5 mM Cu(II) at neutral pH. The initial concentration of CCl_4 was 20 μM, and the pH was maintained at 7.0 $\pm$ 0.1 using 50 mM HEPES buffer.

of the solutions in the presence of various concentrations of Cu(II) at a constant Fe(II) concentration of 3 mM. No obvious dechlorination of CCl_4 by 3 mM Fe(II) was observed in the absence of Cu(II). Addition of low concentrations of Cu(II) significantly enhanced the dechlorination of CCl_4. The dechlorination efficiency of CCl_4 by Fe(II) increased with increasing Cu(II) concentrations ranging from 0.2 to 0.5 mM. Further increase in Cu(II) concentration lowered the dechlorination efficiency of CCl_4, and only 35% of the initial CCl_4 was removed within 12 h when the Cu(II) concentration was increased to 4 mM. This decrease in dechlorination efficiency at high Cu(II) concentrations may be attributed to the decrease in pH values and the increase in redox potentials. As depicted in Figure 1B, the pH value was maintained at 7.0 $\pm$ 0.2 after 12 h within the Cu(II) concentration range of 0−0.5 mM, while the pH value decreased to 5.5 when the concentration was up to 4 mM. In addition, the redox potentials of the solutions increased from −350 mV in the absence of Cu(II) to +100 mV at 4 mM Cu(II). Maithreepala and Doong (*9*) depicted that 4 mol of protons could be released into the solution when 1 mol of Cu(II) reacted with 1 mol of Fe(II). When the Cu(II) concentration increased, the Fe(II) concentration could decrease by oxidizing to Fe(III). Moreover, the hydrolysis of Cu(II) ions can also release protons into the solution to lower the buffer capacity. Because of both the decrease in pH and the oxidation of Fe(II), the redox potential increased and the dechlorination efficiency of CCl_4 decreased (*9*).

Concentration Effect of Fe(II) on CCl_4 Dechlorination in the Presence of 0.5 mM Cu(II). Figure 2 shows the dechlorination of CCl_4 and the production of chloroform ($CHCl_3$) in the presence of various concentrations of Fe(II) and 0.5 mM Cu(II). The dechlorination efficiency of CCl_4 increased from 15% at 0.5 mM to 93% at 2 mM within 24 h. A nearly complete degradation of CCl_4 was observed when the Fe(II) concentration was higher than 1.5 mM, clearly showing that Fe(II) species is the crucial factor controlling the CCl_4 dechlorination efficiency and rate in aqueous solution. The measured ORP values decreased from +106 mV at 0.5 mM Fe(II) to −219 mV at 2 mM Fe(II) and then slowly to −257 mV when the Fe(II) concentration was increased to 5 mM (Figure S1, Supporting Information). Chloroform was identified as the major product of CCl_4 via hydrogenolysis, and the maximum concentrations of 13−14 μM were obtained after the termination of the experiment. This corresponds to 60−70% of CCl_4 dechlorination, which is in good agreement with the reported results (*7*, *27*). Moreover, small peaks of dichloromethane (CH_2Cl_2) and tetrachloroethylene (C_2Cl_4) appeared in the GC-ECD chromatograms. A trace amount of methane in the headspace was also detected by GC−MS when a high concentration of CCl_4 (3 mM) was used in the dechlorination experiment, implying that further dechlorination to the less chlorinated byproducts or non-chlorinated final products was occurred. In addition, several studies showed that CCl_4 could be transformed to carbon monoxide (CO) and formate ($HCOO^-$) via reductive hydrolysis (*1*, *8*, *23*), suggesting that the 30−40% loss of CCl_4 may be due to the formation of formate and carbon monoxide in the liquid phases.

TABLE 1. Concentrations of Acid-Extractable, Dissolved, Surface-Bound, and Fixed Fe(II) in Aqueous Solutions Containing 0.5 mM Cu(II) and Various Initial Concentrations of Fe(II) after 24 h[a]

		concentrations of Fe(II) (mM)					
initial	Fe(II)/Cu(II)[b]	total Fe[c]	acid extractable[d]	dissolved	surface-bound[e]	fixed Fe(II)[f]	Cu(I) (mM)
0.5	1	0.48 ± 0.12	0.23 ± 0.02	0	0.23	0.06	0.21
1.0	2	1.03 ± 0.17	0.26 ± 0.05	0.025 ± 0.03	0.23	0.33	0.41
1.5	3	1.47 ± 0.15	0.33 ± 0.04	0.055 ± 0.02	0.27	0.76	0.41
2.0	4	1.98 ± 0.19	0.75 ± 0.03	0.29 ± 0.06	0.46	0.84	0.41
2.5	5	2.54 ± 0.21	1.03 ± 0.02	0.32 ± 0.05	0.71	1.06	0.41
3.0	6	3.01 ± 0.15	1.30 ± 0.06	0.32 ± 0.04	0.98	1.29	0.41
4.0	8	4.03 ± 0.18	2.11 ± 0.08	0.35 ± 0.07	1.76	2.53	0.42
5.0	10	4.89 ± 0.23	2.96 ± 07	0.35 ± 0.05	2.61	1.61	0.43

[a] The pH of the system was controlled at 7.0 ± 0.1. [b] The molar ratio of initial Fe(II)/Cu(II). [c] The total Fe concentrations determined by ICP−OES. [d] Concentration of 1 M HCl-extractable Fe(II). [e] Surface-bound Fe(II) concentration = acid-extractable Fe(II) − dissolved Fe(II). [f] Fixed Fe(II) = initial Fe(II) − acid extractable Fe(II) + oxidized Fe(II). The oxidized Fe(II) concentration was assumed to be equal to the determined Cu(I) concentration.

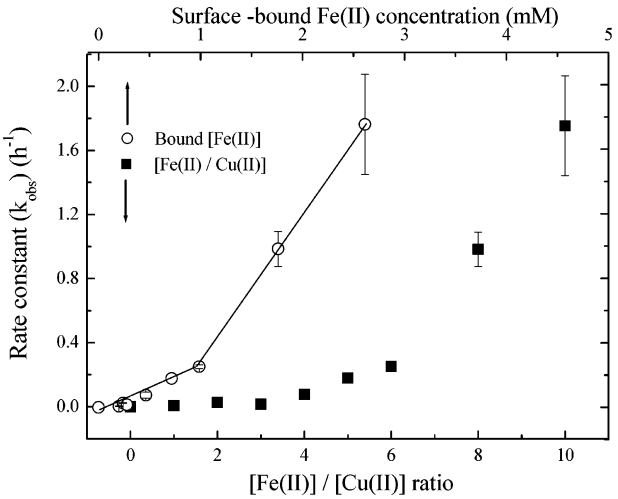

FIGURE 3. Pseudo-first-order rate constant (k_{obs}) for CCl_4 dechlorination as a function of the ratio of [Fe(II)]/[Cu(II)] and the surface-bound Fe(II) concentration in aqueous solutions containing 0.5 mM Cu(II) at neutral pH.

The dechlorination of CCl_4 by Fe(II) in Cu(II)-amended solutions followed pseudo first-order reaction kinetics (*9*):

$$\ln(C_t/C_0) = -k_{obs}t \quad (1)$$

where C_0 and C_t are the concentrations of CCl_4 at the initial time and at time t, respectively, and k_{obs} is the first-order rate constant for CCl_4 dechlorination. The degradation of CCl_4 in Figure 2A showed a clear first-order behavior at concentrations of 3−5 mM. At low Fe(II) concentrations, however, the first-order kinetics was followed only within the initial period of time. It means that the same reaction kinetics assumption for CCl_4 dechlorination will be followed for simplicity at low Fe(II) concentrations. Figure 3 shows the rate constants for CCl_4 dechlorination as functions of the initial and the sorbed Fe(II) concentrations in the presence of 0.5 mM Cu(II) at pH 7. The k_{obs} increased slightly from 0.007 to 0.252 h^{-1} when the initial Fe(II) concentrations increased from 0.5 to 3 mM. Further increase in Fe(II) concentration dramatically increased the dechlorination rate. When the initial Fe(II) concentrations were within the range of 4−5 mM, the k_{obs} for CCl_4 dechlorination was 4−7 times higher than that with 3 mM Fe(II). The increase in k_{obs} at high Fe(II) concentration is probably due to the formation of precipitates when the anoxic solutions contained both Fe(II) and Cu(II) (*9*):

$$2Fe^{2+} + 2Cu^{2+} + 7H_2O \rightarrow Cu_2O + 2Fe(OH)_3 + 8H^+ \quad (2)$$

According to eq 2, amorphous ferrihydrite and cuprous oxide are formed when the molar ratio between Fe(II) and Cu(II) is 1. At high concentrations of Fe(II), the excess ferrous ions would adsorb onto the surfaces of ferric oxides to form surface-bound iron species, which subsequently accelerate the dechlorination rate of CCl_4 at neutral pH.

Table 1 shows the changes in concentrations of dissolved and surface-bound Fe(II) after 24 h of the addition of various concentrations of Fe(II) in the buffered solutions containing 0.5 mM Cu(II). The extractable Cu(I) concentrations at each system are also shown in Table 1. The total extractable Cu(I) concentrations, except those from the 0.5 mM Fe(II)-amended solution, were within the range of 0.41−0.43 mM, implying that similar amounts of ferric oxides were produced. The lower recovery of Cu(I) in the solution with 0.5 mM Fe(II) might be due to the incomplete reduction of Cu(II). In contrast, the surface-bound Fe(II) concentrations increased with increasing initial Fe(II) concentration, which was in a good agreement with the k_{obs}. This means that Fe(II) species plays an important role in the dechlorination rate of CCl_4 in the presence of Cu(II) ions. Previous studies (*6*, *7*, *9*) showed that the reaction rate constant of CCl_4 in an heterogeneous Fe(II)−Fe(III) system followed a linear relationship with respect to the surface-bound Fe(II) concentration. In this study, however, a two-linear phase relationship between the k_{obs} and the surface-bound Fe(II) concentration was observed (Figure 3B), suggesting that the dechlorination of CCl_4 in solutions containing Fe(II) and Cu(II) is controlled not only by the surface-bound Fe(II) concentration but also by other factors such as the molar ratio of Fe/Cu. Several studies have reported that Fe(II) could be fixed to Fe(III)-containing mineral surfaces, resulting in the formation of different morphologies of iron(III) oxides after a relative long contact time (*5*, *28*, *29*). Jeon et al. (*28*) observed the interactions of dissolved Fe(II) with hematite surface that transformed into magnetite ($Fe^{II}Fe_2^{III}O_4$) after a relative long time. Satapanajaru et al. (*30*) also reported that ferrihydrite could react with Fe(II) to form magnetite. In this study, the acid-extractable concentrations of Fe(II) in all batches were lower than the initial concentrations of Fe(II) after 24 h, and the difference in total Fe(II) between the measured and the added amounts increased with increasing initial Fe(II) concentration. This shows the possibility of the fixation of Fe(II) and the change in mineral phase of amorphous ferric oxide to the crystalline ferric oxides at various Fe/Cu ratios.

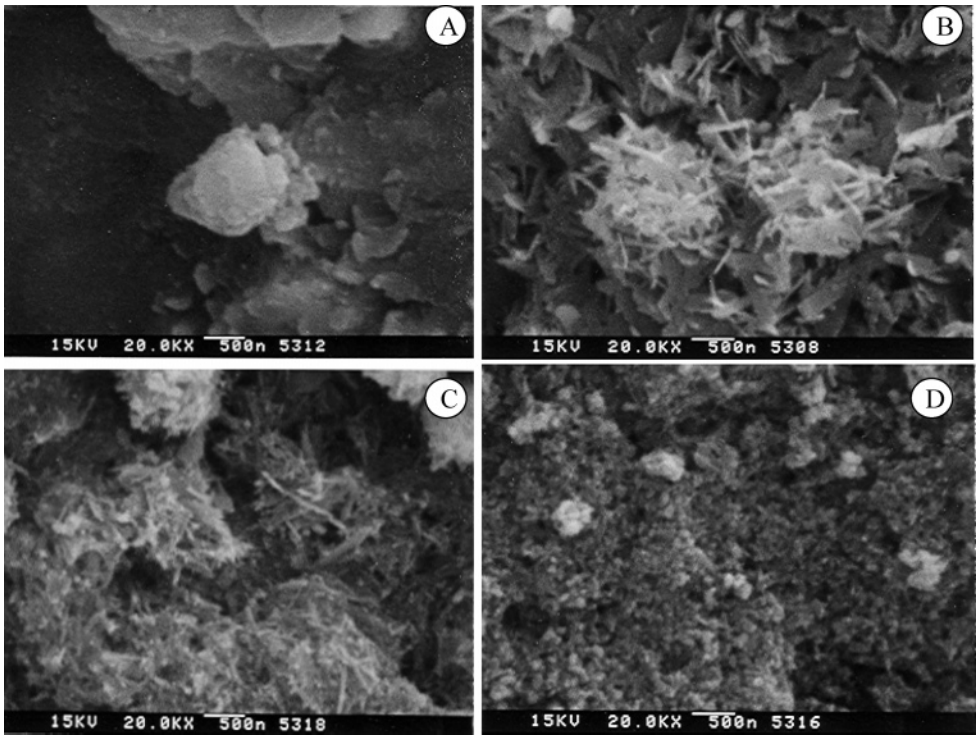

FIGURE 4. SEM images of the precipitates in solutions containing 0.5 mM Cu(II) and various Fe(II) concentrations ranging between 0.5 and 5 mM at neutral pH. The stoichiometric ratios between Fe(II) and Cu(II) were (A) 1:1, (B) 4:1, (C) 6:1, and (D) 10:1. All the precipitates were harvested after 48 h under anoxic conditions.

Change in Morphology of Chemogenic Solids at Various Fe/Cu Ratios. To further understand the change in morphologies of chemogenic solids at various Fe(II)/Cu(II) ratios, SEM and XRPD were used to identify the surface morphology and crystal phase of the precipitates. A high concentration of Cu(II) (3 mM) was used to react with Fe(II) in stoichiometric ratios to generate sufficient amounts of chemogenic solids. Figure 4 shows the SEM images of chemogenic solids at various stoichiometries of Fe/Cu. The surface morphology of the precipitates varied at different Fe/Cu ratios, and the reactive species increased rapidly with increasing concentrations of Fe(II). Ferrihydrite was produced at Fe/Cu ratio of 1, while goethite crystals were clearly shown at Fe/Cu ratios of 4−6 and appeared to encrust a fraction of ferrihydrite with a lath-like habit. The XRPD patterns also showed the change in crystal phases of the chemogenic solids at various Fe/Cu ratios (Figure 5). The major peaks of cuprous oxide (Cu_2O) were observed at 36.42°, 42.22°, and 61.3° (2θ), and no distinct ferric oxide peak was identified at Fe/Cu ratio of 1.0. The SEM image of the Fe(II) and Cu(II) mixture with a similar ratio may represent those minerals (Figure 4A). When the ratio of Fe(II)/Cu(II) increased to 4, at least three morphologies of mineral particles were observed. The peaks in the XRPD pattern (Figure 5) could be assigned to goethite, magnetite, and cuprous oxides. Although the particles were difficult to identify by their shapes, the needlelike particles probably were goethite, which is in agreement with the XRPD results (Figure 5). When the Fe(II)/Cu(II) concentration ratio was increased to 6, the needlelike goethite particles were abundant but with small particle sizes. Goethite is a well-crystallized ferric oxide and has been demonstrated to effectively enhance the dechlorination efficiency and rate of chlorinated compounds by Fe(II) under anoxic conditions (*5*, *7*, *9*). Therefore, the decrease in particle size may increase the surface area to sorb more Fe(II) that can increase the rate and efficiency of CCl_4 dechlorination. Increasing the concentration ratio to 10 changed the morphology of the solids.

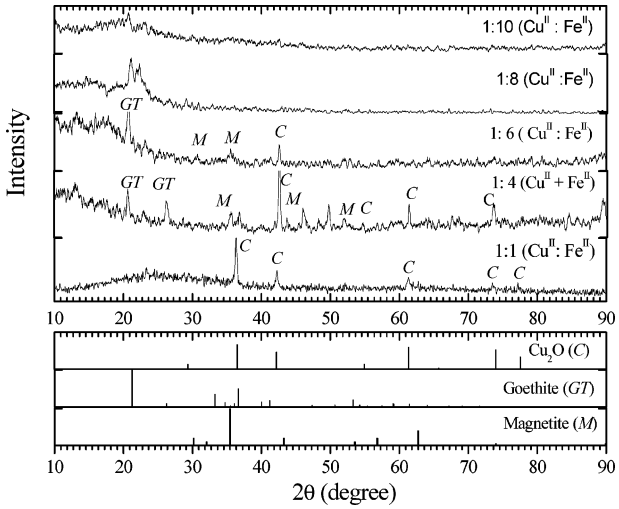

FIGURE 5. XRPD patterns of the solid phases precipitated at various Fe(II)/Cu(II) ratios after 48 h of incubation.

The needlelike particles were not observed in the SEM image (Figure 4D). In addition, no XRD peak related to goethite appeared at the Fe(II)/Cu(II) ratio of 10, revealing that an amorphous mineral phase with small particle sizes was formed.

XRPD patterns at various pH values ranging from 5.5 to 8.5 were also observed at the Fe/Cu ratio of 1 (Figure S2, Supporting Information). This reflects the fact that the precipitates could be produced over a wide pH range and that the Fe/Cu ratio is an important factor controlling the morphology of the precipitates. Several additional peaks, which can be assigned to magnetite and goethite, were observed when the molar ratios of Fe/Cu increased to 4−6 at neutral pH. Recently, Hansel et al. (*31*) observed the formation of goethite and magnetite when biogenic Fe(II) was fixed over ferrihydrite in both column and batch systems.

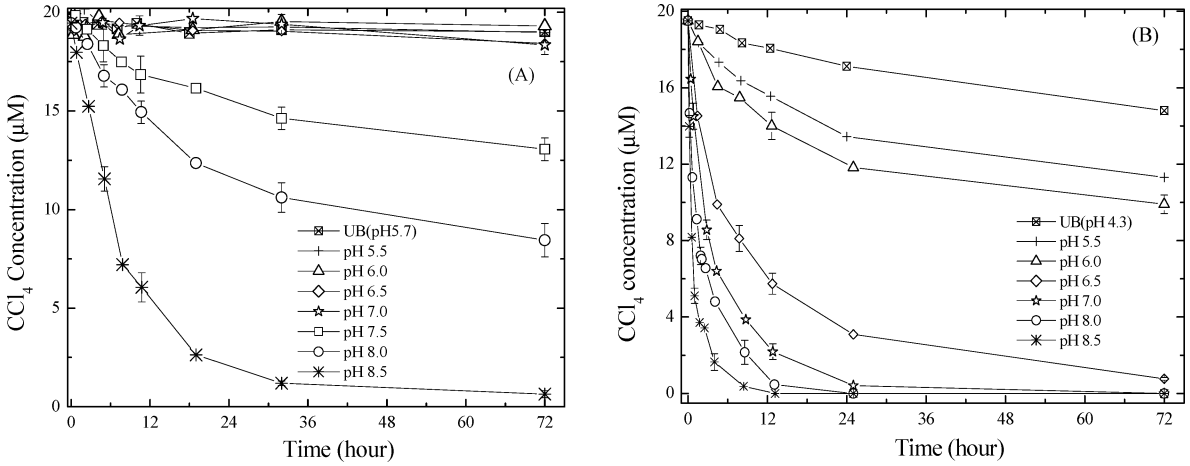

FIGURE 6. Effects of pH on the dechlorination of 20 μM CCl_4 by 3 mM Fe(II) in (A) the absence and (B) the presence of 0.5 mM Cu(II). MES buffer was used to control the pH at 5.0, 5.5 and 6.0. HEPES buffer was used to maintain the pH at 7.0, 7.5, and 8.0. TRIS buffer was used for pH 8.5.

Tolchev et al. (*32*) also found that the chemical composition of precipitates was dependent on the concentration of Fe(II) or $Fe(OH)_2$ in the suspension. These results clearly show that the addition of excess Fe(II) concentrations to solutions containing Cu(II) can form different mineral phases and morphologies of reactive surface-bound Fe(II) species, resulting in an acceleration of the CCl_4 dechlorination rate. However, no distinct peak was observed in XRD patterns when Fe/Cu ratios were increased to 8−10, presumably due to the presence of the amorphous oxides. Baltpurvins et al. (*33*) showed that the phase conversion from ferrihydrite to crystalline ferric oxides was significantly hampered in the presence of chloride ions. In the present study, the amendment of large amounts of Fe(II) as $FeCl_2$ increased the concentration of chloride ion in the system and, therefore, may inhibit the formation of crystal minerals. Ferrihydrite has a larger specific surface area than magnetite and goethite. Therefore, the increase in surface-bound Fe(II) species associated with ferrihydrite due to sorption may increase the CCl_4 dechlorination rate at high Fe/Cu ratios.

The mechanism for the formation of crystalline iron(III) oxide in the presence of aqueous Fe(II) and Cu(II) ions is not well understood. Previous studies reported that magnetite can be formed by the oxidation of $Fe(OH)_2$ under neutral or alkaline conditions (*30*) or from the oxidation of green rust (*30*, *34*). The poorly crystalline iron oxides may also be transformed to goethite (*35*). Mann et al. (*36*) reported that green rust could be formed as an intermediate during the conversion of ferrihydrite to magnetite. In this study, a red-brown color appeared at the Fe/Cu ratio of 1, depicting the formation of Cu_2O and amorphous ferrihydrite (eq 2). The red-brown color then slowly changed to green-brown color during the first 12 h when an excess molar concentration of Fe(II) was present. The green color is generally due to the formation of ferrous hydroxides or green rust. $Fe(OH)_2$ is generally formed by reaction of Fe(II) and OH^- ions under basic conditions. During the preequilibrium of 20 h, the color changed gradually to black-brown. This change may be due to the oxidation of ferrous hydroxide to magnetite (eq 3) or the formation of green rust by reacting Fe(II) ions with Fe(III) species (eq 4). However, no green-brown color was observed when the concentrations of Cu(II) and Fe(II) were similar. These results suggest that green rust could be formed as an intermediate and then oxidized to magnetite or goethite (eqs 5 and 6):

$$3Fe(OH)_2 + CCl_4 \rightarrow Fe_3O_4 + CHCl_3 + 2H_2O + HCl \quad (3)$$

$$Fe(OH)_2^+ + 3FeOH^+ + Cl^- + 3OH^- + 2H_2O \rightarrow [Fe^{II}_3Fe^{III}(OH)_8][Cl\cdot 2H_2O] \quad (4)$$

$$6[Fe^{II}_3Fe^{III}(OH)_8][Cl\cdot 2H_2O] + 5CCl_4 \rightarrow 8Fe_3O_4 + 5CHCl_3 + 11HCl + 28H_2O \quad (5)$$

$$2[Fe^{II}_3Fe^{III}(OH)_8][Cl\cdot 2H_2O] + 3CCl_4 \rightarrow 8\alpha\text{-}FeOOH + 3\,CHCl_3 + 5HCl + 4H_2O \quad (6)$$

Effect of pH. The pH may affect the formation of reactive chemogenic solids and the reactivity of surface sites on the Fe(III) mineral surfaces. Therefore, the effect of pH on CCl_4 dechlorination was examined, and the pH was maintained within the range of 5.5−8.5 with appropriate buffers. An unbuffered solution containing 3 mM Fe(II) and 0.5 mM Cu(II) at pH 4.5 was also used for comparison. Parallel experiments in the absence of Cu(II) were also conducted to elucidate the effect of possible precipitates on CCl_4 dechlorination.

Figure 6 shows the effect of pH on the dechlorination of CCl_4 by 3 mM Fe(II) in the absence and presence of 0.5 mM Cu(II). In the absence of Cu(II), no apparent dechlorination of CCl_4 was observed over the pH range of 5.5−7.0 (Figure 6A), which is similar to reported results (*7*). An obvious dechlorination of CCl_4 by Fe(II) occurred under alkaline condition and the k_{obs} for CCl_4 dechlorination increased from 0.0097 h^{-1} at pH 7.5 to 0.0946 h^{-1} at pH 8.5. The concentrations of $CHCl_3$ were within the range of 0.42−14.4 μM, which accounted for up to 71% of CCl_4 dechlorination (Table 2). In contrast to the system without Cu(II), CCl_4 was dechlorinated to $CHCl_3$ over a wide pH range when 0.5 mM Cu(II) was added to the solution. The efficiency and rate of CCl_4 dechlorination increased with increasing pH values, and removal ratios of 26−96% were obtained within the pH range of 4.3−6.5. A nearly complete degradation of CCl_4 was observed after 24 h at neutral and basic pH values. The k_{obs} for CCl_4 dechlorination increased dramatically (150-fold) from 0.0057 h^{-1} at pH 4.3 to 0.856 h^{-1} at pH 8.5, showing that the pH value has a great effect on CCl_4 dechlorination by Fe(II) in the presence of Cu(II).

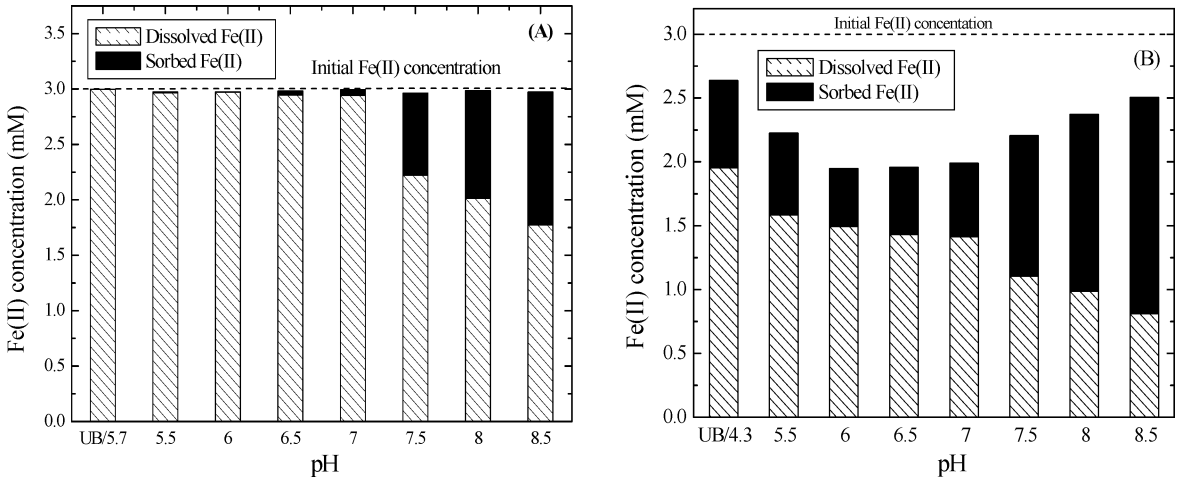

FIGURE 7. Fractions of the dissolved and sorbed concentrations of Fe(II) in (A) the absence and (B) the presence of 0.5 mM Cu(II) at various pH values after 72 h.

TABLE 2. Comparison of the Pseudo-First-Order Reaction Rate Constant (k_{obs}) for CCl_4 Dechlorination by 3 mM Fe(II) and the Production of $CHCl_3$ in the Absence and Presence of 0.5 mM Cu(II) at Various pH Values

	without Cu(II)		with 0.5 mM Cu(II)	
pH	k_{obs} (h^{-1})	max detected $CHCl_3$ (μM)	k_{obs} (h^{-1})	max detected $CHCl_3$ (μM)
UB[a]	0	0.42	0.00571	0.31
5.5	0	0.44	0.0170	0.42
6.0	0	0.41	0.0224	3.93
6.5	0	0.75	0.0827	12.28
7.0	0	0.77	0.252	13.57
8.0	0.0209	8.45	0.347	13.47
8.5	0.0946	14.44	0.856	13.43

[a] The measured pH values of the unbuffered solutions in the presence and absence of 0.5 mM Cu(II) were 5.7 and 4.3, respectively.

The increase in k_{obs} at high pH values may be attributed to the formation of precipitates. Figure 7 illustrates the sorbed and dissolved concentrations of Fe(II) in the presence and the absence of Cu(II) after 72 h. In the solution containing 3 mM Fe(II) without Cu(II), a total Fe(II) concentration of 3 mM was detected in the dissolved fraction at pH 5.5−7.0, showing that no sorbed Fe(II) was present in the solutions. A slight green color was observed when pH values were higher than 7.5. The sorbed Fe(II) accounted for 25−40% of the initial Fe(II) in the solutions at pH 7.5−8.5, which is in a good agreement with the increase in k_{obs}. Previous studies also showed that the increase in dechlorination efficiency of chlorinated compounds at high pH was due to the increasing sorption density of Fe(II) onto iron(III) oxides (*5*, *7*). However, the total Fe(II) concentrations at various pH levels were determined to be 3.0 ± 0.014 mM (n = 8), which was equal to the initial concentration of Fe(II). Previous studies discussed the formation of different Fe(II) species using pH−E_h diagrams (*30*, *37*). The most favorable Fe(II) species in the pH range of 4−6 under anoxic conditions is dissolved Fe(II). Green rust will be formed within the pH range of 6.5−8, while $Fe(OH)_2$ is the most abundant species at high pH values. In this study, the measured ORP value was +180 mV in the unbuffered solution and then gradually decreased to −20 mV at pH 5.5 and to −500 mV at pH 8.5 (Figure S3, Supporting Information). These results suggest that no significant amount of ferric oxide was formed in the absence of Cu(II) and that the sorbed Fe(II) could be green rust or $Fe(OH)_2$.

Unlike the systems without Cu(II), the concentrations of the acid-extractable Fe(II) in the presence of 0.5 mM Cu(II) were lower than 2.5 mM after the termination of dechlorination processes. The Cu(I) concentrations in serum bottles were in the range of 0.44−0.5 mM, and the total Fe concentration determined by ICP−OES was 3.0 ± 0.15 mM (n = 8), clearly showing that the decrease in Fe(II) is mainly due to the formation of ferric oxides. In the unbuffered system where the pH was 4.36 (Figure 7B), sorbed Fe(II) was found but the dechlorination efficiency of CCl_4 was quite low (Figure 6B). This may be due to the protonation of the surface-bound Fe(II) in the acidic pH range. The protonated surface-bound Fe(II) species are less reactive as compared with deprotonated species (*3*). It is noted that the formation of ferric oxide is most prevalent at pH 6.0−7.0 and gradually decreases with increasing pH. The SEM images showed different morphologies of ferric oxides at various pH values due to the fixation of Fe(II) (Figure S4, Supporting Information). In addition to ferric oxides, iron−copper oxides may also be formed. However, such mineral phases were not identified in this study.

Environmental Significance. In natural anoxic environments, several biogeochemical redox processes may take place in parallel, giving rise to several potential reductants for the dechlorination of subsurface contaminants. The Fe(II)−Fe(III) cycle is one of the most important redox processes and could be the dominating removal process for chlorinated contaminants under anoxic conditions. Recently, the impact of transition metals on the reductive dechlorination of chlorinated compounds by structural Fe(II) species has been addressed. Jeong and Hayes (*24*) showed that the addition of transition metal ions including Cu(II), Ni(II), Zn(II), Cd(II), and Hg(II) increased the dechlorination rates of hexachloroethane (HCA) in the presence of mackinawite (FeS). The catalytic activities of Cu(II), Au(III), and Ag(I) in the reduction of chlorinated alkanes by green rust were also demonstrated (*38*, *39*). A possible mechanism for the enhanced CCl_4 reduction is the formation of a galvanic couple involving the zerovalent metal and green rust. Although the concentrations of Cu(II) used in this study are higher than naturally occurring concentrations, our results clearly indicate the potential of using low concentrations of Cu(II) to enhance the dechlorination efficiency and rate of CCl_4 by aqueous Fe(II) in the contaminated subsurface environments. Dissolved Fe(II) can react with Cu(II) to chemically produce different compositions of Fe(III) oxides to accelerate the dechlorination of CCl_4. Several studies (*40*, *41*) have demonstrated the possibility of natural attenuation of CCl_4 in the contaminated aquifers. The observed half-lives for CCl_4 dechlorination range between 5 and 15 d, which are much slower than the results obtained in this study. In contaminated aquifers where Cu(II) and

chlorinated hydrocarbons coexist, ferric oxides are present as alternative electron acceptors by DIRB to reductively dissolute Fe(II). The dissolved Fe(II) can be adsorbed onto the surface of ferric oxides to form the surface-bound Fe(II) species or react with Cu(II) to generate new reactive surface sites for the dechlorination of chlorinated hydrocarbons.

Permeable reactive barriers (PRB) have recently emerged as a possible innovative technology for in situ cleanup of groundwater contamination. Zerovalent iron is the most frequently utilized material, accounting for approximately 45% of PRB applications (*42*). The Fe(II) species generated by the oxidation of metallic iron are also thought to play a key role in the long-term reactivity of metal iron reactive walls for the remediation of aquifers contaminated with chlorinated solvents (*42*−*45*). Several ferric oxides including magnetite, goethite, and green rust have been observed as products during zerovalent iron treatment (*30*, *46*, *47*). Recently, laboratory experimental results showed the effect of transition metal ions including Cu(II) on the dechlorination of chlorinated compounds by zerovalent iron (*48*). The synergistic effect of dissolved Cu(II) and Fe(II) on the reduction of CCl_4 shown in this study may enhance our understanding of the role of Fe(II) and the long-term reactivity of zerovalent iron systems in the dechlorination processes for chlorinated organic contaminants. In conclusion, our results clearly demonstrate the high reactive nature of dissolved Fe(II) in CCl_4 dechlorination in the presence of the Cu(II) ion under anoxic conditions. In the contaminated subsurface, the Fe(II) concentrations can be as high as 1.4−3 mM (*17*). This gives impetus to develop processes that could be used for the coupled detoxification of chlorinated hydrocarbons and metal ions.

Acknowledgments

The authors thank the National Science Council, Taiwan, for the financial support under Contract NSC 92-2211-E-007-001.

Supporting Information Available

Redox potentials as a function of Fe(II) concentration in the presence of 0.5 mM Cu(II) (Figure S1); XRD patterns of the precipitates at various pH values (Figure S2); redox potentials of the Fe(II)-amended aqueous solutions at various pH values in the presence and absence of Cu(II) (Figure S3); SEM images of ferric oxides produced from the reaction of Fe(II) and Cu(II) at various pH values (Figure S4). This material is available free of charge via the Internet at http://pubs.acs.org.

Literature Cited

(1) McCormick, M. L.; Adriens, P. Carbon tetrachloride transformation on the surface of nanoscale biogenic magnetite particles. *Environ. Sci. Technol.* **2004**, *38*, 1045−1053.

(2) Janda, V.; Vasek, P.; Bizova, J.; Belohlav, Z. Kinetic models for volatile chlorinated hydrocarbons removal by zero-valent iron. *Chemosphere* **2004**, *54*, 917−925.

(3) Lee, W.; Batchelor, B. Abiotic, reductive dechlorination of chlorinated ethylenes by iron-bearing soil minerals. 2. Green rust. *Environ. Sci. Technol.* **2002**, *36*, 5348−5354.

(4) Kenneke, J. F.; Weber, E. J. Reductive dehalogenation of halomethanes in iron- and sulfate-reducing sediments. 1. Reactivity pattern analysis. *Environ. Sci. Technol.* **2003**, *37*, 713−720.

(5) Haderlein, S. B.; Pecher, K. Pollutant reduction in heterogeneous Fe(II)-Fe(III) systems. In *Kinetics and Mechanisms of Reactions at the Mineral/Water Interface*; Sparks, D. L., Grundl, T. J., Eds.; ACS Symposium Series 715; Division of Geochemistry, American Chemical Society: Washington, DC, 1998; Chapter 17, pp 342−357.

(6) Kim, S.; Picardal, F. W. Enhanced anaerobic biotransformation of carbon tetrachloride in the presence of reduced iron oxides. *Environ. Toxicol. Chem.* **1999**, *18*, 2142−2150.

(7) Amonette, J. E.; Workman, D. J.; Kennedy, D. W.; Fruchter, J. S.; Gorby, Y. A. Dechlorination of carbon tetrachloride by Fe(II) associated with goethite. *Environ. Sci. Technol.* **2000**, *34*, 4606−4613.

(8) Pecher, K.; Haderlein, S. B.; Schwarzenbach, R. P. Reduction of polyhalogenated methanes by surface-bound Fe(II) in aqueous suspensions of iron oxides. *Environ. Sci. Techol.* **2002**, *36*, 1734−1741.

(9) Maithreepala, R. A.; Doong, R. A. Synergistic effect of copper ion on the reductive dechlorination of carbon tetrachloride by surface-bound Fe(II) associated with goethite. *Environ. Sci. Technol.* **2004**, *38*, 260−268.

(10) Elsner, M.; Schwarzenbach, R. P.; Haderlein, S. B. Reactivity of Fe(II)-bearing minerals toward reductive transformation of organic contaminants. *Environ. Sci. Technol.* **2004**, *38*, 799−807.

(11) O'Loughlin, E. J.; Burris, D. R.; Belcomyn, C. A. Reductive dechlorination of trichloroethene mediated by humic-metal complexes. *Environ. Sci. Technol.* **1999**, *33*, 1145−1147.

(12) Heijman, C. G.; Grieder, E.; Holliger, C.; Swarzenbach, R. P. Reduction of nitroaromatic compounds coupled to microbial iron reduction in laboratory aquifer columns. *Environ. Sci. Technol.* **1995**, *29*, 775−783.

(13) Klausen, J.; Tröber, S. P.; Haderlein, S. B.; Schwarzenbach, R. P. Reduction of substituted nitrobenzenes by Fe(II) in aqueous mineral suspensions. *Environ. Sci. Technol.* **1995**, *29*, 2396−2404.

(14) Vikesland, P. J.; Valentine, R. L. Reaction pathways involved in the reduction of monochloramine by ferrous iron. *Environ. Sci. Technol.* **2000**, *34*, 83−90.

(15) Strathmann, T. J.; Stone, A. T. Abiotic reduction of the pesticides oxamyl and methomyl by Fe(II): Reaction kinetics and mechanism. In *Proccedings of the 219th ACS National Meeting*, Division of Environmental Chemistry, American Chemical Society: Washington, DC, 2000; Vol. 40 (1), pp 141−144.

(16) Hofstetter, T. B.; Heijman, C. G.; Haderlein, S. B.; Holliger, C.; Schwarzenbach, R. P. Complete reduction of TNT and other (poly)nitroaromatic compounds under iron reducing subsurface conditions. *Environ. Sci. Technol.* **1999**, *33*, 1479−1487.

(17) Rügge, K.; Hofstetter, T. B.; Haderlein, S. B.; Bjerg, P. L.; Knudsen, S.; Zraunig, C.; Mosbaek, H.; Christensen, T. Characterization of predominant reductants in an anaerobic leachate-contaminated aquifer by nitroaromatic probe compounds. *Environ. Sci. Technol.* **1998**, *32*, 23−31.

(18) Lovley, D. R. Microbial Fe(III) reduction in subsurface environments. *FEMS Microbiol. Rev.* **1997**, *20*, 305−313.

(19) Tuccillo, M. E.; Cozzarelli, I. M.; Herman, J. S. Iron reduction in the sediments of a hydrocarbon-contaminated aquifer. *Appl. Geochem.* **1999**, *14*, 655−667.

(20) Cui, D.; Eriksen, T. E. Reduction of pertechnetate by ferrous iron in solution: influence of sorbed and precipitated Fe(II). *Environ. Sci. Technol.* **1996**, *30*, 2259−2262.

(21) Buerge, I. J.; Hug, S. J. Influence of mineral surfaces on chromium(VI) reduction by iron(II). *Environ. Sci. Technol.* **1999**, *33*, 4285−4291.

(22) Doong, R. A.; Wu, S. C. Reductive dechlorination of chlorinated hydrocarbons in aqueous-solutions containing ferrous and sulfide ions. *Chemosphere* **1992**, *24*, 1063−1077.

(23) Elsner, M.; Haderlein, S. B.; Kellerhals, T.; Luzi, S.; Zwank, L.; Angst, W.; Schwarzenbach, R. P. Mechanisms and products of surface-mediated reductive dehalogenation of carbon tetrachloride by Fe(II) on goethite. *Environ. Sci. Technol.* **2004**, *38*, 2058−2066.

(24) Jeong, H. Y.; Hayes, K. F. Impact of transition metals on reductive dechlorination rate of hexachloroethane by mackinawite. *Environ. Sci. Technol.* **2003**, *37*, 4650−4655.

(25) Doong, R. A.; Chen, K. T.; Tsai, H. C. Reductive dechlorination of carbon tetrachloride and tetrachloroethylene by zerovalent silicon−iron reductants. *Environ. Sci. Technol.* **2003**, *37*, 2575−2581.

(26) Doong, R. A.; Schink, B. Cysteine-mediated reductive dissolution of poorly crystalline iron(III) oxides by *Geobacter sulfurreducens*. *Environ. Sci. Technol.* **2002**, *36*, 2939−2945.

(27) Diehl, H.; Smith, G. F. *The Copper Reagents*: *Cuproine*, *Neocuproine*, *Bathocuproine*, 2nd ed.; Schilt, A. A., McBride, M., Eds.; The Frederick Smith Chemical Company: Columbus, OH, 1972; pp 33−35.

(28) Jeon, B. H.; Dempsey, B. A.; Burgos, W. D. Kinetics and mechanisms for reactions of Fe(II) with iron(III) oxides. *Environ. Sci. Technol.* **2003**, *37*, 3309−3315.

(29) Jeon, B. H.; Dempsey, B. A.; Burgos, W. D.; Royer, R. A. Reactions of ferrous iron with hematite. *Colloids Surf. A* **2001**, *191*, 41−55.
(30) Satapanajaru, T.; Shea, P. J.; Comfort, S. D.; Roh, Y. Green rust and iron oxide formation influences metolachlor dechlorination during zerovalent iron treatment. *Environ. Sci. Technol.* **2003**, *37*, 5219−5227.
(31) Hansel, C. M.; Benner, S. G.; Neiss, J.; Dohnakova, A.; Kakkudapu, R. K.; Fendorf, S. Secondary mineralization pathways induced by dissimilatory iron reduction of ferrihydrite under advective flow. *Geochim. Cosmochim. Acta.* **2003**, *67*, 2977−2992.
(32) Tolchev, A. V.; Kleschov, D. G.; Bagautdinova, R. R.; Pervushin, V. Y. Temperature and pH effect on composition of a precipitate formed in $FeSO_4$−H_2O−H^+/OH^--H_2O_2 system. *Mater. Chem. Phys.* **2002**, *74*, 336−339.
(33) Baltpurvins, K. A.; Burns, R. C.; Lawrance, G. A.; Stuart, A. D. Effect of pH and anion type on the aging of freshly precipitated iron(III) hydroxide sludges. *Environ. Sci. Technol.* **1996**, *30*, 939−944.
(34) Erbs, M.; Hansen, H. C. B.; Olsen, C. E. Reductive dechlorination of carbon tetrachloride using iron(II) iron(III) hydroxide sulfate (green rust). *Environ. Sci. Technol.* **1999**, *33*, 307−311.
(35) Schwertman, U.; Cornell, R. M. *Iron Oxides in the Laboratory*: *Preparation and Characterization*; VCH Verlagsgsellschschaft mbH: Weinheim, Germany, 1991; pp 61−79.
(36) Mann, S.; Spark, N. H. C.; Couling, S. B.; Larcombe, M. C. Crystallochemical characterization of magnetic spinels prepared from aqueous-solution. *J. Chem. Soc., Faraday Trans. 1* **1989**, *85*, 3033−3044.
(37) Genin, J. M. R.; Bourrié, G.; Trolard, F.; Abdelmoula, M.; Jaffrezic, A.; Refait, P.; Maitre, V.; Humbert, B.; Herbillon, A. Thermodynamic equilibria in aqueous suspensions of synthetic and natural Fe(II)−Fe(III) green rusts: Occurrences of the mineral in hydromorphic soils. *Environ. Sci. Technol.* **1998**, *32*, 1058−1068.
(38) O'Loughlin, E. J.; Kemner, K. M.; Burris, D. R. Effects of Ag−I, Au−III, and Cu−II on the reductive dechlorination of carbon tetrachloride by green rust. *Environ. Sci. Technol.* **2003**, *37*, 2905−2912.
(39) O'Loughlin, E. J.; Burris, D. R. Reduction of halogenated ethanes by green rust. *Environ. Toxicol. Chem.* **2004**, *23*, 41−48.
(40) Devlin, J. F.; McMaster, M.; Barker, J. F. Hydrogeologic assessment of in situ natural attenuation in a controlled field experiment. *Water Resour. Res.* **2002**, *38*, 1−11.
(41) Devlin, J. F.; Katic, D.; Barker, J. F. In situ sequenced bioremediation of mixed contaminants in groundwater. *J. Contam. Hydrol.* **2004**, *69*, 233−261.
(42) Scherer, M. M.; Richter, S.; Valentine, R. L.; Alvarez, J. J. Chemistry and microbiology of permeable reactive barriers for in situ groundwater clean up. *Crit. Rev. Microbiol.* **2000**, *26*, 221−264.
(43) Bonin, P. M. L.; Jedral, W.; Odziemkowski, M. S.; Gillham, R. W. Electrochemical and Raman spectroscopic studies of the influence of chlorinated solvents on the corrosion behaviour of iron in borate buffer and in simulated groundwater. *Corros. Sci.* **2000**, *42*, 11, 1921−1939.
(44) Scherer, M. M.; Balko, B. A.; Tratnyek, P. G. The role of oxides in reduction reactions at the mineral−water interface. In *Kinetics and Mechanisms of Reactions at the Mineral/Water Interface*; Sparks, D. L., Grundl, T. J., Eds.; ACS Symposium Series 715; Division of Geochemistry, American Chemical Society: Washington, DC, 1998; Chapter 17, pp 301−322.
(45) Phillips, D. H.; Gu, B.; Watson, D. B.; Roh, Y.; Liang, L.; Lee, S. Y. Performance evaluation of a zerovalent iron reactive barrier: Mineralogical characteristics. *Environ. Sci. Technol.* **2000**, *34*, 4169−4176.
(46) Ritter, K.; Odziemkowski, M. S.; Gillham, R. W. An in situ study of the role of surface films on granular iron in the permeable iron wall technology. *J. Contam. Hydrol.* **2002**, 87−111.
(47) Odziemkowski, M. S.; Schuhmacher, T. T.; Gillham, R. W.; Reardon, E. J. Mechanism of oxide film formation on iron in simulating groundwater solutions: Raman spectroscopic studies. *Corros. Sci.* **1998**, *40*, 371−389.
(48) Miehr, R.; Tratnyek, P. G.; Bandstra, J. Z.; Scherer, M. M.; Alowitz, M. J.; Bylaska, E. J. Diversity of contaminant reduction reactions by zerovalent iron: Role of the reductate. *Environ. Sci. Technol.* **2004**, *38*, 139−147.

Received for review April 22, 2004. Revised manuscript received September 23, 2004. Accepted September 27, 2004.

ES0493906